THE JOURNAL OF BIOLOGICAL CHEMISTRY VOL. 287, NO. 22, pp. 18562–18572, May 25, 2012

Neuromedin U Type 1 Receptor Stimulation of A-type K^+ Current Requires the $\beta\gamma$ Subunits of G_o Protein, Protein Kinase A, and Extracellular Signal-regulated Kinase 1/2 (ERK1/2) in Sensory Neurons*

Received for publication, November 9, 2011, and in revised form, March 28, 2012 Published, JBC Papers in Press, April 4, 2012, DOI 10.1074/jbc.M111.322271

Yiming Zhang[‡], Dongsheng Jiang[§], Yuan Zhang[‡¶], Xinghong Jiang[‡], Fen Wang[‡], and Jin Tao[‡1]

From the [‡]Department of Neurobiology, Key Laboratory of Pain Research & Therapy, Medical College of Soochow University, Suzhou 215123, China, the [§]Department of Dermatology and Allergic Diseases, University of Ulm, Ulm 89081, Germany, and the [¶]Department of Neurology, The Second Affiliated Hospital of Soochow University, Suzhou 215004, China

Background: Regulation of I_A has an important role in determining the electrical properties of dorsal root ganglion neurons.
Results: Neuromedin U (NMU) increases I_A via NMUR1 that couples to the $\beta\gamma$ subunits of G_o protein, PKA, and ERK.
Conclusion: NMUR1 stimulation of I_A contributes to neuronal hypoexcitability.
Significance: Selective regulation of I_A by G protein-coupled receptors will contribute to neuronal excitability and subsequent transmission of the nociceptive electrical signals.

Although neuromedin U (NMU) has been implicated in analgesia, the detailed mechanisms still remain unclear. In this study, we identify a novel functional role of NMU type 1 receptor (NMUR1) in regulating the transient outward K^+ currents (I_A) in small dorsal root ganglion (DRG) neurons. We found that NMU reversibly increased I_A in a dose-dependent manner, instead the sustained delayed rectifier K^+ current (I_{DR}) was not affected. This NMU-induced I_A increase was pertussis toxin-sensitive and was totally reversed by NMUR1 knockdown. Intracellular application of GDPβS (guanosine 5′-*O*-(2-thiodiphosphate)), QEHA peptide, or a selective antibody raised against the $G\alpha_o$ or $G\beta$ blocked the stimulatory effects of NMU. Pretreatment of the cells with the protein kinase A (PKA) inhibitor or ERK inhibitor abolished the NMU-induced I_A response, whereas inhibition of phosphatidylinositol 3-kinase or PKC had no such effects. Exposure of DRG neurons to NMU markedly induced the phosphorylation of ERK (*p*-ERK), whereas *p*-JNK or *p*-p38 was not affected. Moreover, the NMU-induced *p*-ERK increase was attenuated by PKA inhibition and activation of PKA by foskolin would mimic the NMU-induced I_A increase. Functionally, we observed a significant decrease of the firing rate of neuronal action potential induced by NMU and pretreatment of DRG neurons with 4-AP could abolish this effect. In summary, these results suggested that NMU increases I_A via activation of NMUR1 that couples sequentially to the downstream activities of $G\beta\gamma$ of the G_o protein, PKA, and ERK, which could contribute to its physiological functions including neuronal hypoexcitability in DRG neurons.

Neuromedin U (NMU),[2] a highly conserved peptide, is expressed widely not only in the central nervous system (CNS) (1) but also in peripheral tissues (2). This peptide acting through its receptor has been implicated in regulating a variety of physiological functions, including stress response, energy homeostasis, and nociception (2). Two G protein-coupled receptors including NMU type 1 receptor (NMUR1) and NMUR2 have been identified as the endogenous receptors for NMU (3, 4). NMUR1 is expressed more abundantly in peripheral tissues, whereas NMUR2 is localized more centrally. These distribution patterns suggest that each receptor subtype may have different but specific physiological roles (5). For example, NMU has recently been reported to be involved in spinal nociceptive reflexes (5, 6), and this CNS effect was thought to be mediated by NMUR2, but not NMUR1. In contrast, NMUR1 was shown to decrease the neuronal excitability of peripheral dorsal root ganglion (DRG) (7), rather than the spinal cord neurons (8). Interestingly, NMUR1 was reported to be expressed in small to medium diameter neurons in the peripheral neuronal system (7, 8), whereas NMUR2 was not detectable. These data together suggest that NMUR1 could be involved in NMU-mediated peripheral analgesic effects. Nevertheless, the detailed mechanisms underlying NMUR1 anti-nociception in peripheral neuronal system are still largely unknown and as such require elucidation.

Nociceptive neurons, which are small to medium size (9, 10), consist of several classes that differ in their expression patterns of various ion channels that lead to a functional diversity in

* This work was supported by National Natural Science Foundation of China Grants 30900437 and 81171056, Natural Science Funding of Jiangsu Province Grants BK2009118 and BK2011440, Natural Science Funding for Colleges and Universities in Jiangsu Province Grant 09KJB180008, a grant from the Scientific Research Foundation for the Returned Overseas Chinese Scholars of State Education Ministry (to J. T.), Start-up Funding of Soochow University Grant Q4134901, and Dong-Wu Scholar Funding of Soochow University (to J. T.), and a project funded by the Priority Academic Program Development of Jiangsu Higher Education Institutions.

[1] To whom correspondence should be addressed: 199 Ren-Ai Rd., Suzhou 215123, People's Republic of China. Tel.: 86-512-65880126; Fax: 86-512-65880397; E-mail: taoj@suda.edu.cn.

[2] The abbreviations used are: NMU, neuromedin U; NMUR1, neuromedin U type 1 receptor; I_A, transient outward K^+ currents; Kv, voltage-gated K^+ channels; I_{DR}, sustained delayed rectifier K^+ current; CTX, cholera toxin; PTX, pertussis toxin; G$\beta\gamma$, G-protein $\beta\gamma$ subunits; DRG, dorsal root ganglion; GDPγS, guanosine 5′-*O*-(2-thiodiphosphate); 4-AP, 4-aminopyridine.

sensory neuron signaling (11, 12). Abnormal excitability of neurons is attributable to alterations in the expression and functional characteristics of voltage-gated ion channels such as Na^+, Ca^{2+}, and K^+ (13, 14). In contrast to Na^+ and Ca^{2+} channels, K^+ channel expression in DRG neurons has received attention only recently (15, 16). Voltage-gated K^+ channel (Kv) currents are critical determinants of neuronal excitability in sensory neurons and are divided into two major categories: the transient A-type K^+ currents (I_A) and the sustained delayed rectifier-type K^+ currents (I_{DR}) (10, 17). I_A activates at subthreshold membrane potentials, inactivate rapidly, and rapidly recover from inactivation: these are important characteristics to influence neuronal excitability and to modulate synaptic plasticity (18, 19). For example, down-regulation of I_A in the nociceptors may increase pain sensation (20). As I_A has an important role in determining the electrical properties of DRG neurons, the regulation of I_A will contribute to neuronal excitability (14) and subsequent transmission of the nociceptive electrical signals (20, 21).

In this study, we investigated the effects of NMU on I_A and elucidated the underlying mechanisms in small DRG neurons in mice. Based on pharmacological manipulation of the NMU-induced I_A increase, we report that NMU increased I_A via the $\beta\gamma$ subunits of G_o protein in a PKA-dependent ERK pathway. This I_A increase induced by NMU was mediated by activation of the NMUR1 receptors. One of the immediate outcomes is the induction of neuronal hypoexcitability in the DRG neurons with possible implications in pain processing.

EXPERIMENTAL PROCEDURES

Pharmacological Agents—All drugs were obtained from Sigma, unless otherwise indicated. Stock solutions of NMU, GDPβS, pertussis toxin (PTX), cholera toxin (CTX), PKI 6-22, H-89, 4-aminopyridine (4-AP), $CdCl_2$, and chelerythrine chloride were prepared in distilled deionized water. Stock solutions of U73122, LY294002, U0126, PD98059, forskolin, calphostin C, and GF109203X were prepared in dimethyl sulfoxide. The concentration of dimethyl sulfoxide in the bath solution is expected to be less than 0.01%, and had no functional effects on I_A. An antibody raised against the $G\alpha_o$ protein was a generous gift from Dr. Q. Ma (Institute of Neuroscience, Soochow University). This antibody has been previously shown to specifically recognize the G_o protein but not the G_i subunit (22). The QEHA peptide and SKEE peptide (22) were synthesized by GenScript (NJ).

Isolation of Dorsal Root Ganglion Neurons—All procedures have been approved by the Animal Care and Use Committee of Soochow University and were in compliance with the National Institutes of Health Guide for the Care and Use of Laboratory Animals. Neurons were isolated from lumbar (L_4–L_6) dorsal root ganglia (DRG) of adult mice (ICR, 4–6 weeks) using our previously described methods (7, 23). Briefly, the freshly removed ganglia were minced and enzymatically digested with collagenase I for 30 min (37 °C) and then with trypsin (2.5 mg/ml) for 15 min (37 °C). They were then gently triturated with a fire-polished pipette to obtain a suspension with single cells. Isolated cells were collected by centrifugation and suspended in minimal essential medium supplemented with FBS (10%), B27 (2%), Glutamax (1%), and penicillin/streptomycin (20 units/ml, 0.2 mg/ml). Dissociated neurons were plated on polylysine (0.1 mg/ml)-coated glass coverslips and kept in 95% air and 5% CO_2 incubators at 37 °C until recording. Isolated DRG neurons were recorded within 24–48 h after plating.

Electrophysiological Recordings—For electrophysiological recording, only small-sized DRG neurons (soma diameter 20–27 μm) were selected. Whole cell patch-clamp recordings were performed at room temperature (22–24 °C) with a Multi-Clamp 700B amplifier (Molecular Devices, USA). Recording pipettes (WPI) had ~3 MΩ resistance when filled with internal solution. pClamp 10.2 was used to acquire and analyze data. A-type K^+ currents were recorded in voltage-clamp mode. Signals were filtered at 1 kHz and digitized at 10 kHz. Series resistance (Rs) and capacitance (Cm) values were taken directly from readings of the amplifier after electronic subtraction of the capacitive transients. Series resistance was compensated to the maximum extent possible (at least 75%). Current traces were corrected with on-line P/6 trace subtraction. Multiple independently controlled glass syringes served as reservoirs for a gravity-driven local perfusion system. Solution exchange was accomplished by constant suction through a glass capillary tube at the opposite end of the recording dish. For voltage-clamp experiments, the internal solution contained (mM): KCl 140, $CaCl_2$ 0.5, $MgCl_2$ 1, EGTA 5, HEPES 10, Mg_2ATP 3, and Na_2GTP 0.3, pH adjusted to 7.4 with KOH (295 mosM). The external solution contained (in mM): choline-Cl 150, KCl 5, $CaCl_2$ 0.03, HEPES 10, $MgCl_2$ 1 and Glucose 10, pH adjusted to 7.4 with KOH (310 mosM). To record K_V currents, Na^+ in control external solution was replaced with equimolar choline and the Ca^{2+} concentrations were reduced to 0.03 mM to suppress Ca^{2+} currents and prevent Ca^{2+} channels becoming Na^+ conducting (24). The reduced external Ca^{2+} would also be expected to suppress Ca^{2+}-activated K^+ current. For current-clamp and Na^+ current recordings, the pipette solution contained the following (in mM): KCl 110, NaCl 10, EGTA 2, HEPES 25, Mg-ATP 4, and Na_2GTP 0.3, adjusted to pH 7.3 with KOH. The external solution contained (in mM): NaCl 128, KCl 2, $CaCl_2$ 2, $MgCl_2$ 2, glucose 30, HEPES 25, pH adjusted to 7.4 with NaOH. We blocked the sustained delayed rectifier K^+ current (I_{DR}) and voltage-gated Ca^{2+} channels, respectively, by application of 25 mM triethanolamine (25) and 100 μM $CdCl_2$ in the external solution for current clamp recordings. Electrophysiological analysis was performed as previously described (26, 27). In experiments in which neurons were dialyzed with compounds (antibody or peptides), current measurements were started at least 5 min after breaking the patch.

Protein Kinase A (PKA) Activity Assay—Cells were seeded in 12-well plates and pretreated with either vehicle (0.1% dimethyl sulfoxide) or NMU for 10 min. The cells were washed with ice-cold phosphate-buffered saline and placed on ice. 200 μl of lysis buffer (20 mM MOPS, 50 mM β-glycerolphosphate, 50 mM sodium fluoride, 1 mM sodium vanadate, 5 mM EGTA, 2 mM EDTA, 1% Nonidet P-40, 1 mM dithiothreitol, 1 mM benzamidine, 1 mM phenylmethylsulfonyl fluoride, 10 μg/ml of leupeptin, and 10 μg/ml of aprotinin) was added. After a 10-min incubation on ice, the cells were scraped off and transferred to microcentrifuge tubes. The cell lysates were centrifuged for 15

min and aliquots of the supernatants containing 0.2 μg of protein were assayed for PKA activity according to the manufacturer's instructions using an enzyme-linked immunosorbent assay (ELISA) kit (JC Bio-Tec).

Western Blot Analysis—Western blot analysis was performed following the procedure as described previously (7, 23). For antibody detection, after incubation with 5% nonfat milk in TBST for 1 h at room temperature, membranes were then incubated with diluted primary antibody rabbit anti-mouse NMUR1 (Santa Cruz, 1:500), *p*-ERK1/2 (Santa Cruz, 1:1000), *p*-JNK (Santa Cruz, 1:1000), *t*-JNK (Santa Cruz, 1:1000), *p*-p38 (Santa Cruz, 1:1000), or *t*-p38 (Santa Cruz, 1:1000) at 4 °C. After 5 washes with TBST, membranes were incubated for 2 h with goat anti-rabbit secondary antibody (Sigma, 1:5000). After 5 washes, the specific binding of the primary antibody was detected with SuperSignal Ultra chemiluminescent substrate (Pierce).

siRNA Transfection in DRG Neurons—The cells were seeded at high density onto laminin-polyornithine-coated coverslips. The NMUR1 siRNAs (sense, 5′-GCCUCAGUCAACUAACUGUTT-3′, antisense, 5′-ACAGUUAGUUGACUGAGGCTT-3′) were purchased from Genepharm (Shanghai, China). The siRNA sequences were subjected to BLAST analysis to exclude potential off-target effects. The negative control siRNA (5′-UUCUCCGAACGUGUCACGUTT-3′) was used as control. DRG neurons were transfected with 0.6 μg of siRNA (100 nM final concentration, chemical modification with 6-FAM) using Oligofectamine (Invitrogen). After 24 h post-transfection, small DRG neurons that fluoresced green as observed under the inverted fluorescence microscope (Ti-2000, Nikon) were selected for whole cell patch clamp analysis.

Immunofluorescent Staining of NMUR1—DRG neurons were grown on polylysine-coated coverslips, and fixed in phosphate-buffered saline (PBS) containing 4% sucrose and 4% paraformaldehyde (PFA) for 20 min at 4 °C. The fixed cells were washed three times with PBS before permeabilization in PBS containing 0.1% Triton X-100 for 5 min. Nonspecific staining was blocked by 4% goat serum in PBS for 1 h. Slides were incubated with primary antibody rabbit anti-mouse NMUR1 (Santa Cruz, 1:500) for 1 h at room temparature. After washing three times with PBS, Alexa Fluor 488-conjugated chicken anti-rabbit IgG (green) was applied to the samples at a dilution of 1:500. The slides were examined by using a laser-scanning confocal microscope (Fluoview BX61, Olympus). Negative controls, omitting each primary antibody, were performed in each case and no significant staining was observed (data not shown).

Data Analysis—All data are presented as mean ± S.E., and GraphPad Prism software was used for data plotting. Treatment effects were statistically analyzed by one-way analysis of variance followed by Bonferroni's multiple comparison test. Paired or two-sample *t* test was used when comparisons were restricted to two means. Error probabilities of $p < 0.05$ were considered statistically significant. Concentration-response curves were fitted by the sigmoidal Hill equation: $I/I_{control} = 1/(1 + 10^{(\log IC50\text{-}X)n_H})$, where X is the decadic logarithm of the concentration used, IC_{50} is the concentration at which the half-maximum effect occurs, and nH is the Hill coefficient. The membrane conductance (G) at each command potential (V_m) was determined by dividing the measured membrane current (I) by the driving force as follows: $G = I/(V_m - E_K)$, where E_K is the equilibrium K^+ potential and was calculated to be −76 mV. Activation data (G-V curve) were fitted by the following modified Boltzmann equation: $G/G_{max} = 1/\{1 + \exp[-(V_{½} - V_m)/k]\}$, where G_{max} is the fitted maximal conductance, $V_{½}$ is the membrane potential for half-activation, and k is the slope factor. Steady-state inactivation of I_A was fitted with the following negative Boltzmann equation: $I/I_{max} = 1/\{1 + \exp[-(V_{½} - V_m)/k]\}$, where I_{max} is maximal current.

RESULTS

NMU Selectively Increases I_A in Small DRG Neurons—There were two main types of outward voltage-gated K^+ channel (Kv) currents described in nociceptive DRG neurons: the transient A-type K^+ current (I_A) and the sustained delayed rectifier K^+ current (I_{DR}) (24, 28). To begin dissecting the roles of NMU in modulation of I_A in small (soma diameter 20–27 μm) DRG neurons, we first isolated these two kinetically different Kv currents in these neurons. With Na^+ and Ca^{2+} currents eliminated (see "Experimental Procedures"), a large outward current was evoked by a command potential of +40 mV from a holding potential of −80 mV in small DRG neurons (Fig. 1*A*). The typical current profile observed in these neurons exhibited a rapidly inactivating component along with a sustained component. A 150-ms prepulse to +10 mV allowed the transient channels to inactivate, leaving only the I_{DR} (Fig. 1*A*, left). Subtraction of I_{DR} from the total current yields a transient I_A (Fig. 1*A*, *right*). The I_A could be blocked by application of 5 mM 4-AP (increase % = 82.4 ± 2.3%, $n = 7$), which further confirmed effective I_A isolation.

Bath application of 1 μM NMU increased I_A by 26.2 ± 1.8% in small DRG neurons (Fig. 1, *B* and *D*), whereas I_{DR} was not significantly affected (Fig. 1, *C* and *D*). Upon washout of NMU, the amplitude of I_A partially returned to the pre-treatment level within 3 min (Fig. 1*B*). Using the magnitude of the effect that NMU has on I_A elicited by depolarization to +40 mV, it is clear that NMU increased I_A in a dose-dependent manner (Fig. 1*E*). The relationship between the concentration of NMU used and the degree of increase observed is described by a logistic equation where the concentration of NMU producing the half-maximal increase (IC_{50}) is 0.32 μM, the apparent Hill coefficient is 0.91, and the maximal incremental effect is 28.8 ± 2.6% (Fig. 1*E*). To further identify the selective I_A increase induced by NMU, we investigated whether 4-AP, a classic I_A blocker, would abrogate NMU-mediated response. Indeed, application of 5 mM 4-AP abrogated the NMU-induced I_A increase in small DRG neurons (Fig. 1*F*). Notably, application of NMU during the maximum 4-AP-induced response failed to produce any further inhibition (Fig. 1*F*).

NMU Rightward Shifts Steady-state Inactivation Curve—As a dose-dependent increase in the peak current density of I_A was evident, we next determined whether the biophysical properties of I_A were affected by NMU. The current-voltage (I-V) curves showed that 1 μM NMU significantly increased I_A at each tested voltage from −10 mV, and peaked at +40 mV where the current density increased from 209.3 ± 22.8 to 288.1 ± 25.6 pA/pF ($n = 9$, $p < 0.01$, Fig. 2, *A* and *B*). We next

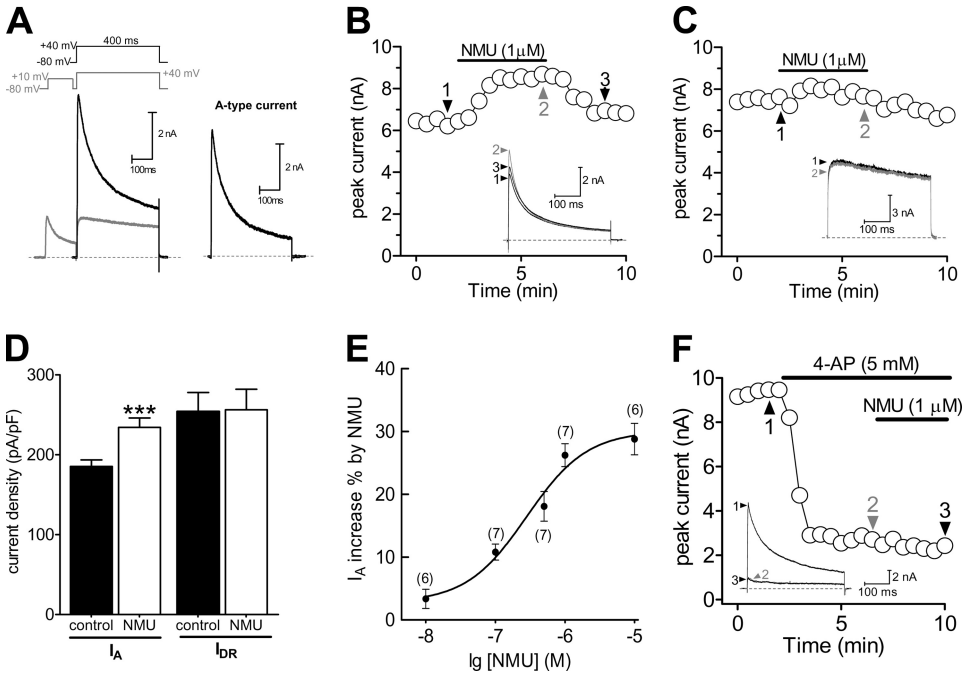

FIGURE 1. **NMU selectively increased I_A in small DRG neurons.** *A*, isolation of I_A. Na^+ currents, Ca^{2+} currents, and Ca^{2+}-activated K^+ currents have been eliminated (see "Experimental Procedures"). *Left,* the membrane voltage was held at −80 mV and I_A was isolated by a two-step voltage protocol. *Right,* the remaining current after off-line subtraction of the noninactivating portion of current remaining after the prepulse to −10 mV. This protocol is used for isolation of I_A in all figures. *B* and *C*, representative current traces and the time course showed that I_A ($n = 7$, *B*), but not sustained delayed rectifier K^+ current (I_{DR}) ($n = 9$, *C*), was significantly increased during exposure to 1 μM NMU. *D,* summary data of current density showed that 1 μM NMU selectively increased I_A. *E,* dose-response curve for the stimulatory effects of NMU on I_A. The *line* represents the best fit of the data points to the sigmoidal Hill equation. Number of cells tested at each concentration of NMU is indicated in *parentheses*. *F,* time course and exemplary traces showed no effect of 1 μM NMU on I_A in the presence of 4-AP ($n = 5$). ***, $p < 0.001$ *versus* control.

analyzed the voltage dependence of activation and inactivation potentials and first observed a slight but statistically insignificant shift of 1.3 mV in the hyperpolarized direction of the activation potential ($V_{½}$ from −9.7 ± 1.3 to −10.2 ± 1.6 mV, and k value from 20.5 ± 1.8 to 19.9 ± 1.4, $n = 7$) (Fig. 2*C*). In contrast, NMU at 1 μM significantly shifted the steady-state inactivation potentials of I_A channels in the depolarizing direction by ~12 mV ($V_{½}$ from −49.5 ± 1.8 to −37.6 ± 1.1 mV, $p < 0.05$; and k value from 11.7 ± 0.7 to 16.4 ± 1.1, $p < 0.05$) (Fig. 2*D*), which suggest that the increase in I_A observed upon application of NMU in mouse DRG neurons could be due to a decreased proportion of channels remaining in the inactivated state.

NMUR1 Knockdown Blocked NMU-induced I_A Increase—Previous reports including ours have clearly shown the localization of NMUR1, but not NMUR2, in both small- and medium-sized DRG neurons (7, 29). To obtain further evidence that the NMU-induced I_A increase was via NMUR1, first we examined the subcellular expression of NMUR1 in small DRG neurons. Fig. 3*A* clearly showed the membrane localization of NMUR1 in small-sized DRG neurons. Negative controls omitting the primary antibody showed no background (not shown). To determine whether the NMU-induced I_A increase was mediated via NMUR1, we used a siRNA knockdown approach to examine the effect of NMU on I_A in NMUR1-silenced small DRG neurons. Western blot analysis showed that expression of NMUR1 was significantly reduced in cells transfected with NMUR1 siRNA compared with cells transfected with the control siRNA (Fig. 3*B, ctrl siRNA*). As shown in Fig. 3*C*, knockdown of NMUR1 in small DRG neurons resulted in a near complete elimination of NMU enhancement of I_A (Fig. 3*C*), whereas NMU still robustly increased I_A in the control siRNA-transfected cells (Fig. 3, *C* and *D*). These results together suggested that NMU increased I_A via activation of NMUR1 in small DRG neurons in mice.

NMUR1-mediated I_A Increase Requires Gβγ Subunits of G_o Protein—NMUR1 belongs to a large family of G protein-coupled receptors (2, 30, 31). To investigate whether heterotrimeric G proteins are involved in the NMUR1-mediated I_A response, we dialyzed small DRG neurons with GDPβS (1 mM), a nonhydrolysable GDP analog. GDPβS completely abolished the increase of I_A induced by 1 μM NMU (increase % = 3.1 ± 0.8, Fig. 4, *A* and *B*), indicating that G protein activation was required for NMU action. We further determined which isoform of Gα was involved in this inhibition. First, we examined the effects of NMU on I_A in the presence of CTX, which inactivates $G\alpha_s$ by ADP-ribosylation. After pretreatment of DRG neurons with CTX (0.5 μg/ml), NMU (1 μM) still robustly increased I_A (increase % = 23.6 ± 2.1, Fig. 4, *A* and *B*), which indicated that the increase of I_A was $G\alpha_s$ independent. However, pretreatment of the cells with PTX (0.2 μg/ml), which catalyzes the ADP-ribosylation of $G\alpha_{i/o}$, abolished the stimulatory effect of NMU (increase % = 3.7 ± 1.0, Fig. 4, *A* and *B*). The increase of I_A induced by NMU was sensitive to PTX, but not CTX, indicating that $G\alpha_{i/o}$, but not $G\alpha_s$, was involved. Furthermore, an antibody that specifically binds G_o but not the G_i subunit (27) was used to determine which subtype of G protein was involved in the NMU response. This antibody abolished the increase of NMU on I_A (increase % = 1.5 ± 1.7, Fig. 4, *A* and *B*)

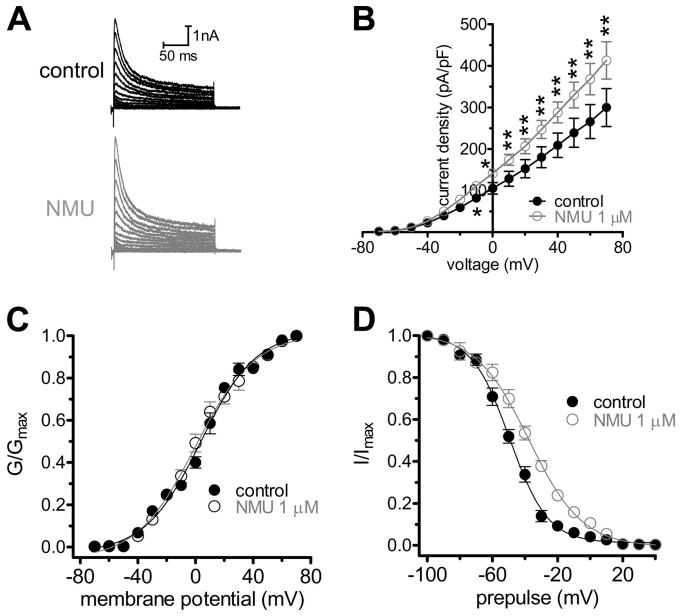

FIGURE 2. **Effects of NMU on biophysical properties of I_A.** *A*, representative current traces of I_A recorded before and after exposure to 1 μM NMU. *B*, current-voltage (I-V) curve in the absence ($n = 9$) and presence ($n = 9$) of 1 μM NMU. *C*, the steady-state activation of I_A channels is not altered by 1 μM NMU ($n = 9$). The voltage-dependent activation of the I_A component; as determined by measuring the peak current amplitude elicited by depolarizing test pulses. The conductance at each voltage was calculated normalized to the conductance determined at +40 mV, and plotted *versus* the test voltage. To determine the voltage dependence of activation, voltage steps of 400 ms were applied at 5-s intervals in +10 mV increase to a maximum of +70 mV. *D*, NMU at 1 μM rightward shifted the steady-state inactivation curve of I_A ($n = 7$). To determine the steady-state inactivation, conditioning prepulses ranging from −100 to +40 mV were applied at 5-s intervals in +10 mV increments for 150 ms followed by a voltage step to +40 mV for 500 ms. *, $p < 0.05$ *versus* control, **, $p < 0.01$ *versus* control.

without significantly altering the current amplitude in the absence of agonist. The denatured G_o-specific antibody (increase % = 26.8 ± 2.3, Fig. 4*B*) and a G_i-specific antibody (increase % = 23.9 ± 3.7, not shown) had no such effect. These results suggested that a G_o-, but not G_i-like protein, was involved in the NMU-mediated response. We further determined the implication of the native G protein $\beta\gamma$ subunit ($G\beta\gamma$) of G_o in the NMU-mediated response. These subunits were quenched in two ways. First, a synthetic peptide, QEHA (200 μM) (26, 32), which competitively binds $G\beta\gamma$ and blocks $G\beta\gamma$-mediated signaling, was introduced into the recording pipette (Fig. 4*B*). Second, a $G\beta$ subunit-specific antibody was applied in the pipette (Fig. 4*B*). We found that either anti-$G\beta$ or QEHA, but not its scrambled peptide SKEE (Fig. 4*B*), abolished the stimulatory effect of NMU on I_A, which suggested that the $G\beta\gamma$ subunit of G_o was necessary for the NMUR1-mediated I_A increase.

PKA Was Involved in NMUR1-mediated I_A Increase—Because NMU appeared to increase I_A via the $\beta\gamma$ subunits of the G_o protein, we further determined the downstream intracellular signaling molecules. Previous studies suggested that the immediate downstream mediator of $G\beta\gamma$ was phosphatidylinositol 3-kinase (PI3K) (32). However, we found that the PI3K inhibitor LY294002 failed to affect the I_A increase induced by NMU (increase % = 25.5 ± 2.3, Fig. 5*A*). G_o protein activation was reported to activate PKC via PLC in cerebellar Purkinje neurons (32). We therefore pretreated DRG neurons with the PLC inhibitor U73122 (3 μM) and found that the NMU-mediated stimulatory effect was not affected by the PLC inhibitor (increase % = 24.9 ± 2.5, Fig. 5*A*). As it has also been reported that PKC could be PLC independently activated (32), we investigated whether the stimulatory effects of NMU were mediated by a PKC-dependent pathway. Preincubation of mouse DRG neurons with PKC inhibitors, GF109203X (1 μM, increase % = 26.1 ± 3.4, Fig. 5*A*) or chelerythrine chloride (1 μM, increase % = 24.6 ± 3.1, Fig. 5*A*), did not significantly affect the I_A increase induced by NMU. A similar result was obtained with another PKC inhibitor, calphostin C (50 nM, increase % = 27.6 ± 2.9, Fig. 5*A*). Previous studies have shown that $G\beta\gamma$ could stimulate PKA activity via regulation of adenylate cyclase types II and V (33, 34). Therefore, we determined whether PKA was involved in the NMU-induced I_A increase and found that small DRG neurons pretreated with a PKA inhibitor, H89 (1 μM), almost completely abolished the NMU-induced I_A increase (increase % = 1.7 ± 0.5, Fig. 5*A*). In contrast, H85 (1 μM), a structurally related but inactive analog, had no such effect (not shown). The PKA dependence of the NMU-induced I_A increase was further validated by dialyzing the cells with a pipette solution containing PKI 6-22, another PKA inhibitor. Our results showed that intracellular application of PKI 6-22 (1 μM) via the recording pipette solution blocked the NMU-induced I_A increase (increase % = 1.3 ± 1.1, Fig. 5*A*). These results suggest that $G\beta\gamma$-dependent PKA was involved in the NMUR1-mediated I_A increase. As a complementary test of our hypothesis, we further investigated whether forskolin, a potent PKA activator, would also induce the I_A increase. Indeed, application of 20 μM forskolin to DRG neurons mimicked the NMU-induced I_A increase (increase % = 17.9 ± 1.3, Fig. 5*B*). In addition, effects of NMU on the PKA activity in DRG neurons were also detected. As shown in Fig. 5*C*, treatment with 1 μM NMU for 10 min resulted in a ~2.3-fold increase of PKA activity in DRG neurons. Knockdown of NMUR1 in DRG neurons resulted in a near complete elimination of the NMU-stimulated PKA activity (Fig. 5*C*). These findings further support the conclusion that the NMUR1-mediated I_A increase in small DRG neurons occurs through a G_o protein $\beta\gamma$ subunit-mediated PKA pathway.

ERK Signaling Was Involved in NMUR1-mediated I_A Increase—ERK/mitogen-activated protein kinase (MAPK) pathway has been demonstrated to play a crucial role in pain regulation. Activation of the MAPK pathway was reported to regulate I_A in dorsal horn neurons (35). It was therefore of interest to examine whether the MAPK signaling pathway is involved in the NMU-induced I_A increase. Western blot analysis showed that exposure of DRG neurons to NMU (1 μM) markedly increased the expression of phosphorylation of ERK (*p*-ERK) (Fig. 6*A*), whereas *p*-JNK (Fig. 6*B*) and *p*-p38 (Fig. 6*C*) remain unchanged, which suggested that ERK could be involved in a NMU-induced response such as I_A regulation. As a complementary test of our hypothesis, knockdown of NMUR1 inhibited the NMU-induced *p*-ERK expression increase. In contrast, the NMU-induced phosphorylation of ERK was not affected by control siRNA treatment (Fig. 6, *D* and *E*). In addition, pretreatment of cells with both the PKA antagonist as well as the MAPK/ERK kinase (MEK) inhibitor U0126 (20 μM) eliminated NMU-induced ERK activation (Fig. 6, *D* and *E*). We next investigate whether ERK activation was exactly involved in the NMU-in-

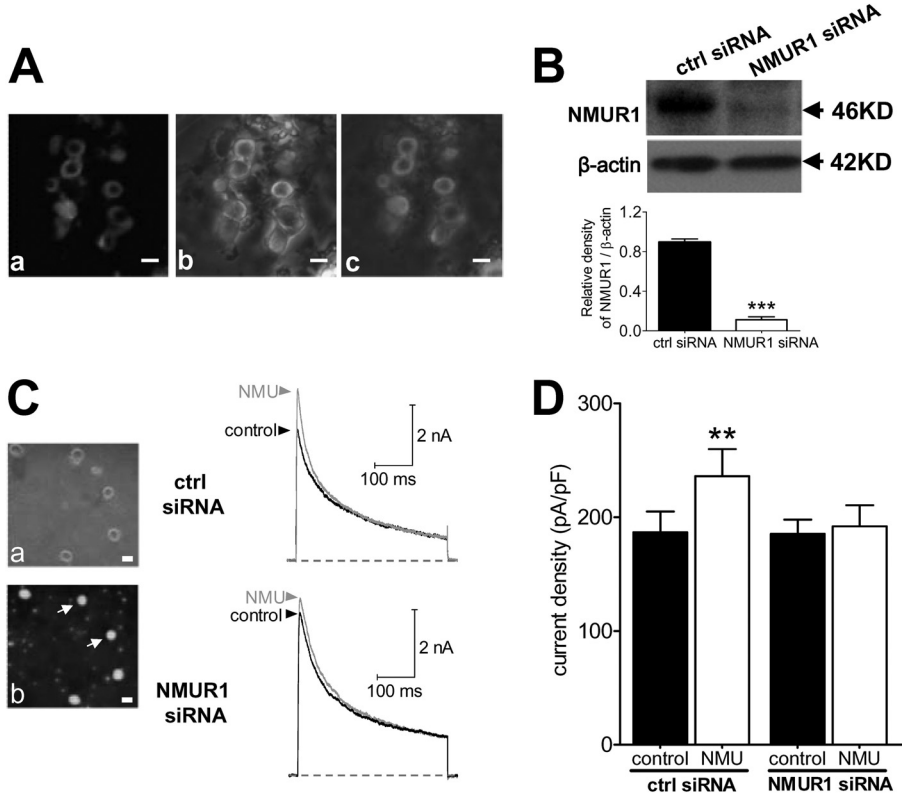

FIGURE 3. **NMU-mediated response is prevented by NMUR1 knockdown.** *A,* membrane expression of NMUR1 determined by confocal microscopy. *a*, fluorescent signals of NMUR1. *b,* differential interference contrast images. *c,* merged picture. *Scale bar*, 25 μm. *B,* protein expression of NMUR1 (46 kDa) was measured using Western blot analysis in control siRNA (*ctrl siRNA*) and NMUR1 siRNA-treated groups. β-Actin (42 kDa) showed the equal loading. *C*, *left,* photomicrographs of phase-contrast (*a*) and fluorescent images (*b*) of small DRG neurons transfected with the NMUR1 siRNA. *Scale bar*, 20 μm. *Right,* representative current traces showed the effects of control siRNA or NMUR1 siRNA on the NMU-induced I_A increase. *D*, summary data showed the effects of control siRNA ($n = 8$) or NMUR1 siRNA ($n = 9$) on the 1 μM NMU-induced I_A increase in small DRG neurons. **, $p < 0.01$ *versus* control.

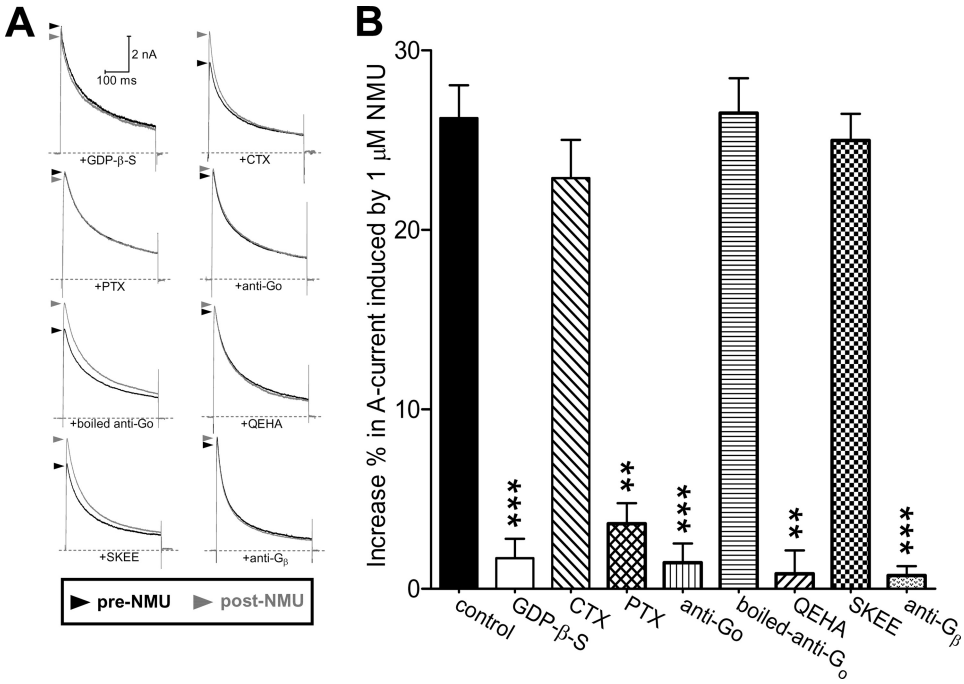

FIGURE 4. **NMUR1-mediated I_A increase requires the G$\beta\gamma$ subunits of G_o protein.** *A* and *B,* representative current traces (*A*) and summary data (*B*) showed the effects of 1 μM NMU on I_A in the presence of GDPβS (1 mM, intracellular applied, $n = 7$), CTX (0.5 μg/ml for 24 h pretreatment, $n = 9$), PTX (0.2 μg/ml for 24 h pretreatment, $n = 9$), anti-G_o (intracellular applied, $n = 7$), boiled anti-G_o (intracellular applied, $n = 5$), QEHA (200 μM, intracellular applied, $n = 9$), SKEE (200 μM, intracellular applied, $n = 7$), or anti-G_β (intracellular applied, $n = 8$), respectively. **, $p < 0.01$ *versus* control; ***, $p < 0.001$ *versus* control.

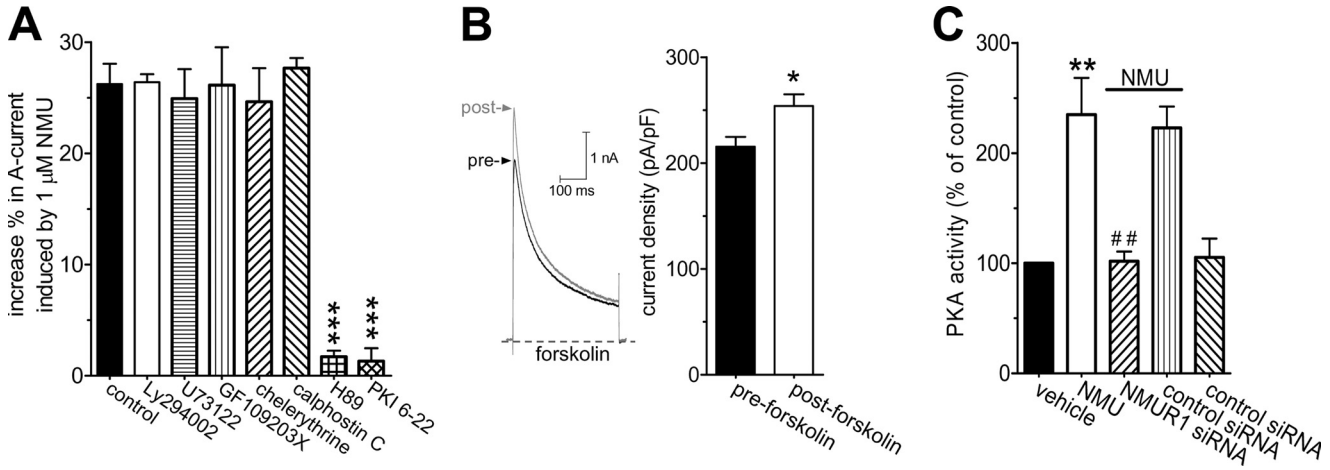

FIGURE 5. **NMUR1-mediated I_A increase was PKA-dependent.** *A,* summary data showed the increase of I_A induced by 1 μM NMU in the presence of LY294002 (3 μM for 30 min, $n = 9$), U73122 (3 μM for 30 min, $n = 9$), GF109203X (1 μM for 30 min, $n = 8$), chelerythrine chloride (1 μM for 30 min, $n = 7$), calphostin C (50 nM, $n = 7$), H89 (1 μM for 30 min, $n = 9$), and PKI 6-22 (1 μM, intracellular applied, $n = 7$), respectively. *B,* representative current traces (*left*) and summary data (*right*) showed the effects of 20 μM forskolin on the peak amplitude of I_A in small DRG neurons ($n = 9$). *C,* NMU increased PKA activity via NMUR1. Cells were treated with either vehicle (control) or 1 μM NMU for 10 min and assayed for PKA activity as described under "Experimental Procedures." The PKA activity data are normalized to the vehicle-treated cells as 100%. *, $p < 0.05$ *versus* control; **, $p < 0.01$ *versus* control; ##, $p < 0.001$ *versus* NMU groups.

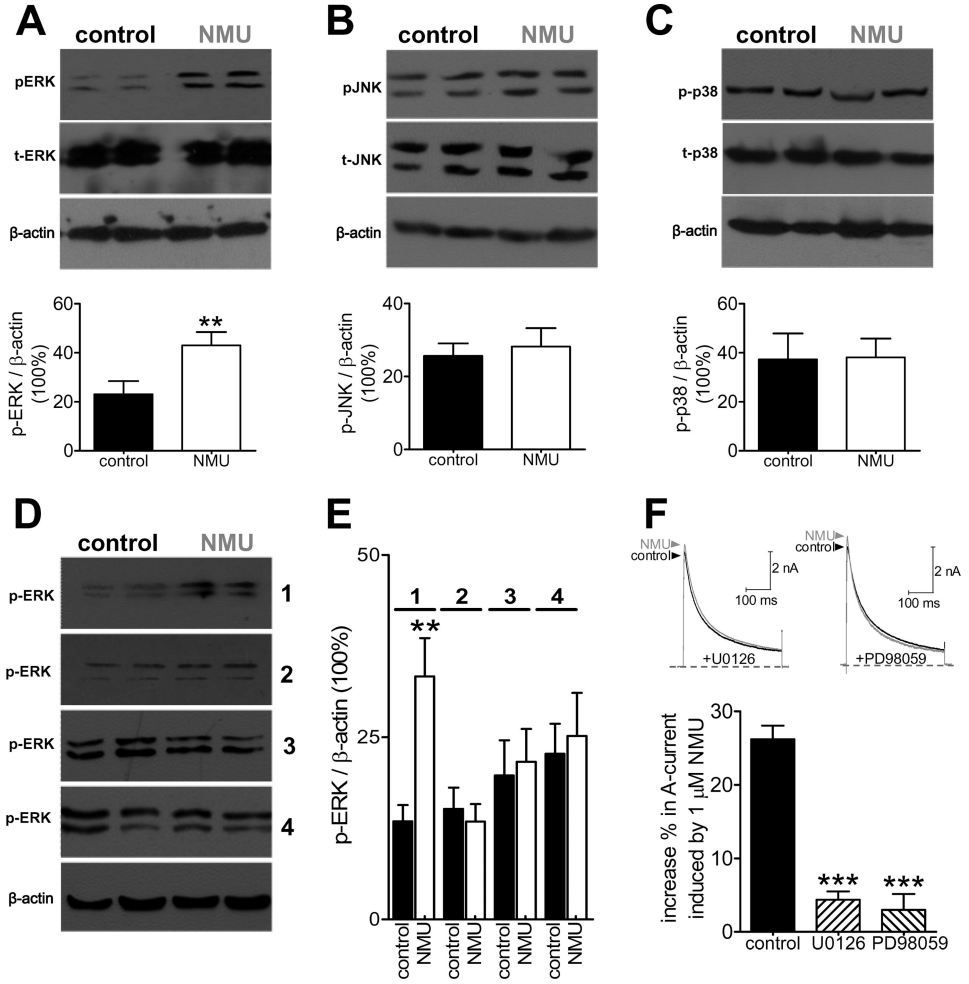

FIGURE 6. **NMU-induced I_A increase involves activation of ERK.** *A–C,* NMU induced increased phosphorylation of ERK (*p*-ERK, A) in DRG neurons, whereas the protein expression levels of *p*-JNK (*B*) or *p*-38 (*C*) were not affected. β-Actin showed equal loading. *D* and *E,* NMU-induced *p*-ERK increase was abolished by NMUR1 knockdown and pretreatment of the cells with PD98059 or H89. Exposure of DRG neurons to NMU still increased *p*-ERK expression in cells transfected with control siRNA. All experiments were performed in triplicate with similar results. *Inset,* numbers *1–4* represents control siRNA, NMUR1 siRNA, H89, and PD98059, respectively. *F,* representative current traces (*upper*) and summary data (*lower*) showed the effects of 1 μM NMU on I_A in the presence of U0126 ($n = 9$) or PD98059 ($n = 7$). **, $p < 0.01$ *versus* control; ***, $p < 0.01$ *versus* control.

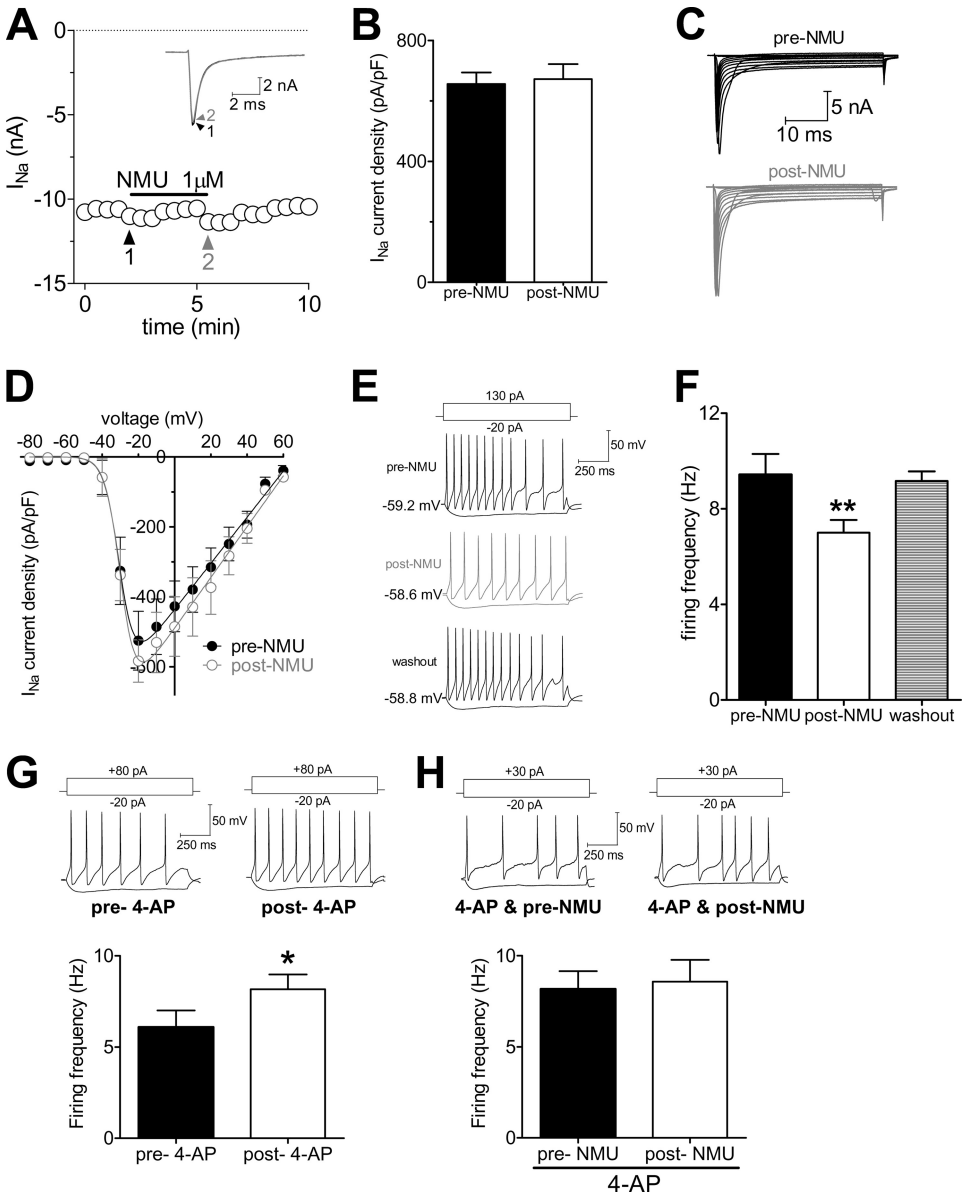

FIGURE 7. **NMUR1 induces neuronal hypoexcitability in small DRG neurons.** *A* and *B,* time course and summary data showed that NMU had no effects on voltage-gated Na^+ channel currents ($n = 6$). *Inset,* representative examples of Na^+ currents recorded before and after application of 1 μM NMU. *C* and *D,* exemplary current traces and current-voltage plot of current density of Na^+ current *versus* test voltage recorded before ($n = 7$) and after ($n = 7$) 1 μM NMU. *E,* representative traces of firing at the resting membrane potential under control conditions, during exposure to 1 μM NMU, and washout. *F,* summary data comparing the average firing rates under the conditions indicated in *panel E* ($n = 14$). Cells were given +130 pA current injections. *G,* representative traces and summary data showed the effects of 4-AP on neuronal firing ($n = 11$). *H,* representative traces and summary data showed 4-AP abolished 1 μM NMU-induced hypoexcitability in small DRG neurons ($n = 17$). *, $p < 0.05$ *versus* pre-drug; **, $p < 0.01$ *versus* pre-drug.

duced I_A increase. We applied U0126, the inhibitor of mitogen-activated ERK kinase (the upstream activator of ERK), to small DRG neurons. Preincubation of the cells with U0126 abrogated the I_A increase induced by NMU (increase % = 3.3 ± 0.5, Fig. 6*F*), whereas U0124, a negative control analog of U0126, elicited no such effects (not shown). Similar results were obtained with another MAPK inhibitor, PD98059 (increase % = 2.6 ± 0.9, Fig. 6*F*). These results together suggest that activation of NMUR1 increase I_A via activation of ERK in mouse DRG neurons.

NMU Decreases Neuronal Excitability in Small DRG Neurons—Kv currents including I_A and I_{DR} in primary sensory neurons are important for regulating neuronal excitability (20, 36). To further address the functional implication of the I_A increase induced by NMUR1, we tested the effects of NMU on membrane excitability in small DRG neurons. We first investigated whether voltage-gated Na^+ channels would be regulated by NMU and found that NMU failed to affect Na^+ current density in small DRG neurons (Fig. 7, *A* and *B*). As shown in Fig. 7, *C* and *D*, the current-voltage (I-V) curves were not shifted. Therefore, by using an external solution including $CdCl_2$ to block the voltage-gated Ca^{2+} channels and triethanolamine to block the I_{DR}, we found that 1 μM NMU significantly decreased the rate of firing to 51.56 ± 6.53% (Fig. 7, *E* and *F*). Upon washout of NMU, the rate of firing was restored (Fig. 7, *E* and *F*). In addition, NMU at 1 μM significantly decreased the AP amplitude and

TABLE 1

Membrane properties of small DRG neurons in mice induced by 1 μM NMU in the absence (−) or presence (+) of 4-AP

Cm, capacitance; R_{in}, input resistance; RMP, resting membrane potential; AHP, afterhyperpolarization potential; FSL, First spike latency; *n*, number of cells (*, $p < 0.05$ *versus* pre-NMU).

a)

NMU		Cm (pF)	R_{in} (mΩ)	RMP (mV)	Rheobase (pA)	AP amplitude (mV)	AP half width (ms)	AP threshold (mV)	FSL (ms)	n
(−)	pre-	20.4±2.5	879.6±73.5	-54.3±2.9	94.3±10.1	89.1±5.7	5.1±0.2	-21.6±1.1	23.1±3.1	14
4-AP	post-	19.6±1.7	938.3±92.7	-53.3±2.4	97.8±8.8	78.7±4.8*	5.2±0.3	-20.5±1.3	29.5±3.2*	14

b)

NMU		Cm (pF)	R_{in} (mΩ)	RMP (mV)	Rheobase (pA)	AP amplitude (mV)	AP half width (ms)	AP threshold (mV)	FSL (ms)	n
(+)	pre-	22.6±2.3	879.6±73.5	-51.3±3.6	77.2±4.9	114.3±5.9	5.9±0.4	-25.6±2.1	18.33±2.2	17
4-AP	post-	21.3±1.9	938.3±92.7	-51.9±3.5	82.8±7.6	110.4±4.9	5.6±0.3	-26.2±2.4	19.2±2.9	17

prolonged the first spike latency. Other membrane properties of neuronal excitability including threshold and resting membrane potential were not significantly changed by NMU (1 μM) in small DRG neurons (Table 1). To further verify that this NMU-induced hypoexcitability was via the I_A increase, we examined the effects of NMU on neuronal excitability with application of 4-AP in the external solution ($n = 17$ neurons, Fig. 7, *G* and *H*) and found that pretreatment of cells with 4-AP completely abolished NMU-induced hypoexcitability in small DRG neurons (Fig. 7*H*). Other membrane properties of neuronal excitability are shown in Table 1. These results together demonstrated that activation of NMUR1 by NMU induces neuronal hypoexcitability via an increase of I_A in small DRG neurons.

DISCUSSION

Our present study adds a new piece of information to the NMUR1 signaling pathway by demonstrating that activation of NUMR1 stimulates A-type K^+ currents (I_A) via the $\beta\gamma$ subunits of the G_o protein and PKA-dependent ERK1/2 pathway and leads to a decrease in neuronal excitability in mouse peripheral sensory DRG neurons, whereas I_{DR} remains unchanged.

Unlike G_i, which inhibits adenylyl cyclase, the main function of G_o can be interpreted through the actions of a common pool of $G\beta\gamma$ dimers (37, 38). Consistently, we have found that the $G\beta\gamma$ subunits of G_o are involved in the NMUR1-mediated I_A increase, because: 1) the response is abolished by dialyzing cells with an anti-G_o antibody; 2) intracellular application of an antibody raised against $G\beta$ or a $G\beta\gamma$ blocking peptide, QEHA, abolishes the NMUR1-mediated response. A known target of $G\beta\gamma$ is PI3K, which has been shown to regulate voltage-gated Ca^{2+} channels via PI3K (39). Our previous study has found that in hippocampus neurons the inhibition of L-type Ca^{2+} channel currents by NMUR1 signaling is mediated by the PI3K-dependent novel PKC pathway (22). However, in the present study, both PI3K inhibitor LY294002 (3 μM), and PKC inhibitors including calphostin C (50 nM) or GF109203 (1 μM) or chelerythrine chloride (1 μM) have no significant effect in DRG neurons, whereas both PKA inhibitors H89 (1 μM) and PKI 6-22 (1 μM) show remarkable suppression of the NMU-induced I_A increase. The difference of downstream pathways utilized by NMUR1 in hippocampal neurons and DRG neurons is likely due to the different origins of the neuron tissues, which have quite different functions. This type of difference has been documented previously. For example, stimulation of dopamine D1 receptor suppresses the slowly inactivating K^+ current via PKA in rat medial prefrontal cortex pyramidal neurons (40), whereas activation of the dopamine D1 receptor inhibits T-type Ca^{2+} channel currents via direct $G\beta\gamma$ binding (41). In addition, the differences in tissue-specific alternative splice variants of ion channels could lead to the activation of different signaling pathways and result in different responses according to the different tissue functions and microenvironment. For example, mutually exclusive splicing patterns in the Cav2.2 gene modulate N-type channel function in nociceptors, leading to a change in morphine analgesia (42). Furthermore, alternative splicing of the Cav1.3 channel IQ domain generates a molecular switch for Ca^{2+}-dependent inactivation within auditory hair cells (43).

PKC-mediated responses are also shown to be tissue specific. For example, activation of PKC by PMA inhibits I_A in dendrites of hippocampal CA1 pyramidal neurons (44), but enhances I_A amplitude in rat cerebellar granule cells (45). In addition, the regulation of I_A could be PKC independent, as reported in murine proximal colonic myocytes (46). In the present study, we have found that in mouse DRG neurons the stimulatory effects of NMU on I_A are PKC independent, but rather are mediated by PKA followed by ERK/MAPK. In pyramidal neuron dendrites, activation of ERK leads to reduction of Kv4.2-encoded I_A via phosphorylation of Thr-607 in the C-terminal of Kv4.2 (47). However, we have found that in mouse small DRG neurons I_A increases after NMUR1 activation and subsequent ERK phosphorylation. This effect is NMUR1 and ERK dependent, because it is blocked by NMUR1 siRNA or MAPK inhibitor PD98059. Although the discrepancy remains to be further clarified, this could be possibly explained by a distinct ERK phosphorylation site or a different Kv subtype encoding I_A in DRG neurons, in which Kv1.4, Kv3.4, Kv4.2, and Kv4.3 channels are endogenously expressed (48). An alternative hypothesis is that ERK phosphorylates an intermediate protein, that in turn up-regulates the I_A currents in DRG neurons. Furthermore, different KCHIP1 splice variants are able to generate different, even opposite modulation of Kv4 channel currents (49).

A-type K^+ channels, the key components controlling membrane excitability (50), have been implicated in the delay of the spike onset (first spike latency) and the decrease in the firing frequency of central neurons (51). Changes in membrane excitability of DRG neurons can directly influence pain symptoms such as hyperalgesia and allodynia *in vivo* (52). An important consequence of the I_A current is to delay the first-spike firing in response to small depolarization (53). Consistent with the NMU-induced I_A increase, activation of NMUR1 in small DRG neurons does lead to an inhibition of neuronal excitability including decreasing spike frequency and increasing first-spike latency, which are the two major parameters that determine the timing of neurotransmitter release, and hence pain transmission (54). Our current study is consistent with our previous reports that NMU induced the membrane hypoexcitability in peripheral sensory neurons. In DRG neurons, both T-type Ca^{2+} channel currents (7) and I_A are regulated by $G\beta\gamma$-dependent PKA activation, downstream of NMUR1 signaling. The stimulation of I_A and inhibition of T-currents both lead to

hypoexcitability. The divergent signals are not contradictory to each other; rather this may imply an additive or even a synergistic effect of NMUR1 in controlling the membrane excitability of DRG neurons. This view is supported by the evidence that T-type Ca^{2+} channels and Kv4 channels can form a signaling complex in rat cerebellar stellate cells that efficiently couples Ca^{2+} influx to KChIP3 to modulate the Kv4 function (55). Although whether the Cav3-Kv4 signaling complex exists in mouse small DRG neurons remains to be further investigated, this interaction may be critical for allowing Kv4 channels encoding I_A to function in the subthreshold membrane potential range to regulate neuronal firing properties.

In summary, this study discovers a novel function of NMU in regulation of I_A in mouse small DRG neurons, whereas the I_{DR} remains unchanged. Based on pharmacological manipulation of the NMU-induced I_A increase, we have identified a second messenger pathway initiated by NMUR1 that couples sequentially to the $\beta\gamma$ subunits of the G_o protein, PKA, and ERK. The NMUR1-mediated I_A increase contributes to its physiological functions including neuronal hypoexcitability. These results suggest that NMUR1 signaling could be a potential therapeutic target for clinical management of pain. However, as several subtypes of Kv channels could underlie I_A in small DRG neurons (56), further studies by using anatomical and genetic approaches are necessary to identify the exact Kv subunits that underlie I_A, and mediate the NMUR1-dependent regulation of I_A in DRG neurons.

Acknowledgment—We thank Dr. Tuck Wah Soong for invaluable advice on the manuscript.

REFERENCES

1. Brighton, P. J., Szekeres, P. G., and Willars, G. B. (2004) Neuromedin U and its receptors. Structure, function, and physiological roles. *Pharmacol. Rev.* **56,** 231–248
2. Budhiraja, S., and Chugh, A. (2009) Neuromedin U, physiology, pharmacology, and therapeutic potential. *Fundam. Clin. Pharmacol.* **23,** 149–157
3. Raddatz, R., Wilson, A. E., Artymyshyn, R., Bonini, J. A., Borowsky, B., Boteju, L. W., Zhou, S., Kouranova, E. V., Nagorny, R., Guevarra, M. S., Dai, M., Lerman, G. S., Vaysse, P. J., Branchek, T. A., Gerald, C., Forray, C., and Adham, N. (2000) Identification and characterization of two neuromedin U receptors differentially expressed in peripheral tissues and the central nervous system. *J. Biol. Chem.* **275,** 32452–32459
4. Shan, L., Qiao, X., Crona, J. H., Behan, J., Wang, S., Laz, T., Bayne, M., Gustafson, E. L., Monsma, F. J. Jr., and Hedrick, J. A. (2000) Identification of a novel neuromedin U receptor subtype expressed in the central nervous system. *J. Biol. Chem.* **275,** 39482–39486
5. Mitchell, J. D., Maguire, J. J., and Davenport, A. P., (2009) Emerging pharmacology and physiology of neuromedin U and the structurally related peptide neuromedin S. *Br. J. Pharmacol.* **158,** 87–103
6. Moriyama, M., Furue, H., Katafuchi, T., Teranishi, H., Sato, T., Kano, T., Kojima, M., and Yoshimura, M. (2004) Presynaptic modulation by neuromedin U of sensory synaptic transmission in rat spinal dorsal horn neurones. *J. Physiol.* **559,** 707–713
7. Wang, F., Zhang, Y., Jiang, X., Zhang, Y., Zhang, L., Gong, S., Liu, C., Zhou, L., and Tao, J. (2011) Neuromedin U inhibits T-type Ca^{2+} channel currents and decreases membrane excitability in small dorsal root ganglia neurons in mice. *Cell Calcium* **49,** 12–22
8. Yu, X. H., Cao, C. Q., Mennicken, F., Puma, C., Dray, A., O'Donnell, D., Ahmad, S., and Perkins, M. (2003) Pro-nociceptive effects of neuromedin U in rat. *Neuroscience* **120,** 467–474
9. Petersen, M., and LaMotte, R. H. (1991) Relationships between capsaicin sensitivity of mammalian sensory neurons, cell size, and type of voltage-gated calcium currents. *Brain Res.* **561,** 20–26
10. Gold, M. S., Dastmalchi, S., and Levine, J. D. (1996) Co-expression of nociceptor properties in dorsal root ganglion neurons from the adult rat *in vitro*. *Neuroscience* **71,** 265–275
11. Cardenas, C. G., Del Mar, L. P., and Scroggs, R. S. (1995) Variation in serotonergic inhibition of calcium channel currents in four types of rat sensory neurons differentiated by membrane properties. *J. Neurophysiol.* **74,** 1870–1879
12. Petruska, J. C., Napaporn, J., Johnson, R. D., Gu, J. G., and Cooper, B. Y. (2000) Subclassified acutely dissociated cells of rat DRG. Histochemistry and patterns of capsaicin-, proton-, and ATP-activated currents. *J. Neurophysiol.* **84,** 2365–2379
13. Waxman, S. G. (1999) The molecular pathophysiology of pain. Abnormal expression of sodium channel genes and its contributions to hyperexcitability of primary sensory neurons. *Pain* **6,** S133–140
14. Abdulla, F. A., and Smith, P. A. (2001) Axotomy- and autotomy-induced changes in the excitability of rat dorsal root ganglion neurons. *J. Neurophysiol.* **85,** 630–643
15. Rasband, M. N., and Trimmer, J. S. (2001) Developmental clustering of ion channels at and near the node of Ranvier. *Dev. Biol.* **236,** 5–16
16. Passmore, G. M., Selyanko, A. A., Mistry, M., Al-Qatari, M., Marsh, S. J., Matthews, E. A., Dickenson, A. H., Brown, T. A., Burbidge, S. A., Main, M., and Brown, D. A. (2003) KCNQ/M currents in sensory neurons. Significance for pain therapy. *J. Neurosci.* **23,** 7227–7236
17. Yoshimura, N., White, G., Weight, F. F., and de Groat, W. C. (1996) Different types of Na^+ and A-type K^+ currents in dorsal root ganglion neurones innervating the rat urinary bladder. *J. Physiol.* **494,** 1–16
18. Ramakers, G. M., and Storm, J. F. (2002) A postsynaptic transient K^+ current modulated by arachidonic acid regulates synaptic integration and threshold for LTP induction in hippocampal pyramidal cells. *Proc. Natl. Acad. Sci. U.S.A.* **99,** 10144–10149
19. Watanabe, S., Hoffman, D. A., Migliore, M., and Johnston, D. (2002) Dendritic K^+ channels contribute to spike-timing dependent long-term potentiation in hippocampal pyramidal neurons. *Proc. Natl. Acad. Sci. U.S.A.* **99,** 8366–8371
20. Ocaña, M., Cendán, C. M., Cobos, E. J., Entrena, J. M., and Baeyens, J. M. (2004) Potassium channels and pain. Present realities and future opportunities. *Eur. J. Pharmacol.* **500,** 203–219
21. Bailey, T. W., Jin, Y. H., Doyle, M. W., and Andresen, M. C. (2002) Vanilloid-sensitive afferents activate neurons with prominent A-type potassium currents in nucleus tractus solitarius. *J. Neurosci.* **22,** 8230–8237
22. Zhang, Y., Jiang, D., Zhang, J., Wang, F., Jiang, X., and Tao, J. (2010) Activation of neuromedin U type 1 receptor inhibits L-type Ca^{2+} channel currents via phosphatidylinositol 3-kinase-dependent protein kinase Cϵ pathway in mouse hippocampal neurons. *Cell. Signal.* **22,** 1660–1668
23. Zhang, Y., Zhang, L., Wang, F., Zhang, Y., Wang, J., Qin, Z., Jiang, X., and Tao, J. (2011) Activation of M3 muscarinic receptors inhibits T-type Ca^{2+} channel currents via pertussis toxin-sensitive novel protein kinase C pathway in small dorsal root ganglion neurons. *Cell. Signal.* **23,** 1057–1067
24. Xu, G. Y., Winston, J. H., Shenoy, M., Yin, H., and Pasricha, P. J. (2006) Enhanced excitability and suppression of A-type K^+ current of pancreas-specific afferent neurons in a rat model of chronic pancreatitis. *Am. J. Physiol. Gastrointest. Liver Physiol.* **291,** G424–G431
25. Vydyanathan, A., Wu, Z. Z., Chen, S. R., and Pan, H. L. (2005) A-type voltage-gated K^+ currents influence firing properties of isolectin B4-positive but not isolectin B4-negative primary sensory neurons. *J. Neurophysiol.* **93,** 3401–3409
26. Tao, J., Hildebrand, M. E., Liao, P., Liang, M. C., Tan, G., Li, S., Snutch, T. P., and Soong, T. W. (2008) Activation of corticotropin-releasing factor receptor 1 selectively inhibits CaV3.2 T-type calcium channels. *Mol. Pharmacol.* **73,** 1596–1609
27. Tao, J., Zhang, Y., Li, S., Sun, W., and Soong, T. W. (2009) Tyrosine kinase-independent inhibition by genistein on spermatogenic T-type calcium channels attenuates mouse sperm motility and acrosome reaction. *Cell Calcium* **45,** 133–143
28. Akins, P. T., and McCleskey, E. W. (1993) Characterization of potassium currents in adult rat sensory neurons and modulation by opioids and

cyclic AMP. *Neuroscience* **56,** 759–769
29. Howard, A. D., Wang, R., Pong, S. S., Mellin, T. N., Strack, A., Guan, X. M., Zeng, Z., Williams, D. L. Jr., Feighner, S. D., Nunes, C. N., Murphy, B., Stair, J. N., Yu, H., Jiang, Q., Clements, M. K., Tan, C. P., McKee, K. K., Hreniuk, D. L., McDonald, T. P., Lynch, K. R., Evans, J. F., Austin, C. P., Caskey, C. T., Van der Ploeg LH, and Liu, Q. (2000) Identification of receptors for neuromedin U and its role in feeding. *Nature* **406,** 70–74
30. Szekeres, P. G., Muir, A. I., Spinage, L. D., Miller, J. E., Butler, S. I., Smith, A., Rennie, G. I., Murdock, P. R., Fitzgerald, L. R., Wu, H., McMillan, L. J., Guerrera, S., Vawter, L., Elshourbagy, N. A., Mooney, J. L., Bergsma, D. J., Wilson, S., and Chambers, J. K. (2000) Neuromedin U is a potent agonist at the orphan G protein-coupled receptor FM-3. *J. Biol. Chem.* **275,** 20247–20250
31. Fujii, R., Hosoya, M., Fukusumi, S., Kawamata, Y., Habata, Y., Hinuma, S., Onda, H., Nishimura, O., and Fujino, M. (2000) Identification of neuromedin U as the cognate ligand of the orphan G protein-coupled receptor FM-3. *J. Biol. Chem.* **275,** 21068–21074
32. Tao, J., Zhang, Y., Huang, H., and Jiang, X. (2009) Activation of corticotropin-releasing factor 2 receptor inhibits Purkinje neuron P-type calcium currents via $G\alpha_o$-dependent PKCϵ pathway. *Cell. Signal.* **21,** 1436–1443
33. Tang, W. J., and Gilman, A. G. (1991) Type-specific regulation of adenylyl cyclase by G protein $\beta\gamma$ subunits. *Science* **254,** 1500–1503
34. Avidor-Reiss, T., Nevo, I., Levy, R., Pfeuffer, T., and Vogel, Z. (1996) Chronic opioid treatment induces adenylyl cyclase V superactivation. Involvement of G$\beta\gamma$. *J. Biol. Chem.* **271,** 21309–21315
35. Hu, H. J., Glauner, K. S., and Gereau, R. W., 4th (2003) ERK integrates PKA and PKC signaling in superficial dorsal horn neurons. I. Modulation of A-type K^+ currents. *J. Neurophysiol.* **90,** 1671–1679
36. Kim, D. S., Choi, J. O., Rim, H. D., and Cho, H. J. (2002) Down-regulation of voltage-gated potassium channel α gene expression in dorsal root ganglia following chronic constriction injury of the rat sciatic nerve. *Brain Res. Mol. Brain Res.* **105,** 146–152
37. Westfall, T. D., McCafferty, G. P., Pullen, M., Gruver, S., Sulpizio, A. C., Aiyar, V. N., Disa, J., Contino, L. C., Mannan, I. J., and Hieble, J. P. (2002) Characterization of neuromedin U effects in canine smooth muscle. *J. Pharmacol. Exp. Ther.* **301,** 987–992
38. Won, J. H., Park, J. S., Ju, H. H., Kim, S., Suh-Kim, H., and Ghil, S. H. (2008) The α subunit of G_o interacts with promyelocytic leukemia zinc finger protein and modulates its functions. *Cell. Signal.* **20,** 884–891
39. Chung, J. J., Okamoto, Y., Coblitz, B., Li, M., Qiu, Y., and Shikano, S. (2009) PI3K/Akt signaling-mediated protein surface expression sensed by 14-3-3 interacting motif. *FEBS J.* **276,** 5547–5558
40. Dong, Y., and White, F. J. (2003) Dopamine D1-class receptors selectively modulate a slowly inactivating potassium current in rat medial prefrontal cortex pyramidal neurons. *J. Neurosci.* **23,** 2686–2695
41. Wolfe, J. T., Wang, H., Howard, J., Garrison, J. C., and Barrett, P. Q. (2003) T-type calcium channel regulation by specific G-protein $\beta\gamma$ subunits. *Nature.* **424,** 209–213
42. Andrade, A., Denome, S., Jiang, Y. Q., Marangoudakis, S., and Lipscombe, D. (2010) Opioid inhibition of N-type Ca^{2+} channels and spinal analgesia couple to alternative splicing. *Nat. Neurosci.* **13,** 1249–1256
43. Shen, Y., Yu, D., Hiel, H., Liao, P., Yue, D. T., Fuchs, P. A., and Soong, T. W. (2006) Alternative splicing of the $Ca_v1.3$ channel IQ domain, a molecular switch for Ca^{2+}-dependent inactivation within auditory hair cells. *J. Neurosci.* **26,** 10690–10699
44. Hoffman, D. A., and Johnston, D. (1998) Down-regulation of transient K^+ channels in dendrites of hippocampal CA1 pyramidal neurons by activation of PKA and PKC. *J. Neurosci.* **18,** 3521–3528
45. Hu, C. L., Zeng, X. M., Zhou, M. H., Shi, Y. T., Cao, H., and Mei, Y. A. (2008) Kv 1.1 is associated with neuronal apoptosis and modulated by protein kinase C in the rat cerebellar granule cell. *J. Neurochem.* **106,** 1125–1137
46. Choi, S., Parajuli, S. P., Lim, G. H., Kim, J. H., Yeum, C. H., Yoon, P. J., and Jun, J. Y. (2006) Imipramine inhibits A-type delayed rectifier and ATP-sensitive K^+ currents independent of G-protein and protein kinase C in murine proximal colonic myocytes. *Arch. Pharm. Res.* **29,** 998–1005
47. Schrader, L. A., Birnbaum, S. G., Nadin, B. M., Ren, Y., Bui, D., Anderson, A. E., and Sweatt, J. D. (2006) ERK/MAPK regulates the Kv4.2 potassium channel by direct phosphorylation of the pore-forming subunit. *Am. J. Physiol. Cell Physiol.* **290,** C852–861
48. Yang, E. K., Takimoto, K., Hayashi, Y., de Groat, W. C., and Yoshimura, N. (2004) Altered expression of potassium channel subunit mRNA and α-dendrotoxin sensitivity of potassium currents in rat dorsal root ganglion neurons after axotomy. *Neuroscience* **123,** 867–874
49. Van Hoorick D, Raes, A., Keysers, W., Mayeur, E., and Snyders, D. J. (2003) Differential modulation of Kv4 kinetics by KCHIP1 splice variants. *Mol. Cell Neurosci.* **24,** 357–366
50. Hu, H. J., Carrasquillo, Y., Karim, F., Jung, W. E., Nerbonne, J. M., Schwarz, T. L., and Gereau, R. W., 4th (2006) The Kv4.2 potassium channel subunit is required for pain plasticity. *Neuron* **50,** 89–100
51. Pongs, O. (1999) Voltage-gated potassium channels. From hyperexcitability to excitement. *FEBS Lett.* **452,** 31–35
52. Zhang, J. M., Song, X. J., and LaMotte, R. H. (1999) Enhanced excitability of sensory neurons in rats with cutaneous hyperalgesia produced by chronic compression of the dorsal root ganglion. *J. Neurophysiol.* **82,** 3359–3366
53. Nisenbaum, E. S., Xu, Z. C., and Wilson, C. J. (1994) Contribution of a slowly inactivating potassium current to the transition to firing of neostriatal spiny projection neurons. *J. Neurophysiol.* **71,** 1174–1189
54. Tolhurst, D. J., Smyth, D., and Thompson, I. D. (2009) The sparseness of neuronal responses in ferret primary visual cortex. *J. Neurosci.* **29,** 2355–2370
55. Anderson, D., Mehaffey, W. H., Iftinca, M., Rehak, R., Engbers, J. D., Hameed, S., Zamponi, G. W., and Turner, R. W. (2010) Regulation of neuronal activity by Cav3-Kv4 channel signaling complexes. *Nat. Neurosci.* **13,** 333–337
56. Chien, L. Y., Cheng, J. K., Chu, D., Cheng, C. F., and Tsaur, M. L. (2007) Reduced expression of A-type potassium channels in primary sensory neurons induces mechanical hypersensitivity. *J. Neurosci.* **27,** 9855–9865